Mucoid morphotype variation of *Burkholderia multivorans* during chronic cystic fibrosis lung infection is correlated with changes in metabolism, motility, biofilm formation and virulence

Running title: Phenotype variation in *B. multivorans* clinical isolates

Content category: Microbial Pathogenicity

Inês N. Silva[2], Ana S. Ferreira[2], Jörg D. Becker[3], James E. A. Zlosnik[4], David P. Speert[4], Ji He[5], Dalila Mil-Homens[2], and Leonilde M. Moreira[1,2*]

[1]Department of Bioengineering, Instituto Superior Técnico (IST), Av. Rovisco Pais, 1049-001 Lisbon, Portugal

[2]IBB- Institute for Biotechnology and Bioengineering, Centre for Biological and Chemical Engineering, IST, Lisbon, Portugal

[3]Instituto Gulbenkian de Ciência, Rua da Quinta Grande Nº 6, 2780-156 Oeiras, Portugal

[4]Division of Infectious and Immunological Diseases, Department of Paediatrics, and Centre for Understanding and Preventing Infection in Children, Faculty of Medicine, University of British Columbia, 950 W 28th Ave, Vancouver BC V5Z 4H4, Canada

[5]Plant Biology Division, the Samuel Roberts Noble Foundation, 2510 Sam Noble Parkway, Ardmore, OK 73401, USA

*Correspondence: Leonilde M. Moreira

Mailing address: Instituto Superior Técnico, Torre Sul, Piso 6, Av. Rovisco Pais, 1049-001 Lisbon, Portugal. Phone: (351)218419031. Fax: (351)218419199. E-mail: lmoreira@ist.utl.pt

Abstract word count: 236

Main text word count: 6661

6 figures and 3 tables

Abbreviations: CF, cystic fibrosis; EPS, exopolysaccharide; *Bcc*, *Burkholderia cepacia* complex

ABSTRACT

Burkholderia cepacia complex (*Bc*c) bacteria are opportunistic pathogens infecting hosts such as cystic fibrosis (CF) patients. *Bc*c long-term infection of CF patient airways has been associated with emergence of phenotypic variation. Here we studied two *Burkholderia multivorans* clonal isolates displaying different morphotypes from a chronically infected CF patient to evaluate traits development during lung infection. Expression profiling of mucoid D2095 and nonmucoid D2214 isolates revealed decreased expression of genes encoding products related to virulence-associated traits and metabolism in D2214. Furthermore, D2214 showed no exopolysaccharide production, lower motility and chemotaxis, and more biofilm formation, particularly under microaerophilic conditions, than the clonal mucoid isolate D2095. When *Galleria mellonella* was used as acute infection model, D2214 at a cell number of approximately $7x10^6$ c.f.u. caused higher survival rate than D2095, although 6 days post-infection most of the larvae were also dead. Infection with the same number of cells by mucoid D2095 caused larvae death by day 4. The decreased expression of genes involved in carbon and nitrogen metabolism may reflect lower metabolic needs of D2214 caused by lack of exopolysaccharide, but also by the attenuation of pathways not required for survival. As a result, D2214 showed higher survival than D2095 in minimal medium for 28-days under aerobic conditions. Overall, adaptation during *Bc*c chronic lung infections give rise to genotypic and phenotypic variation among isolates, contributing to their fitness while maintaining their capacity for survival in this opportunistic human niche.

INTRODUCTION

Burkholderia cepacia complex (*Bc*c) comprises Gram-negative bacteria found in water, soil and associated with plants (Baldwin *et al.*, 2007). They have large genomes (between 7-9 Mbp) and a number of genes ranging from 5500 up to 7900. Due to this high gene content, *Bc*c strains display numerous metabolic enzymes, transporters, regulatory genes and putative virulence determinants, providing them with a great competitive capacity to move between different niches (Holden *et al.*, 2009). *Bc*c bacteria have attracted considerable interest due to infections caused in the airways of cystic fibrosis (CF) patients (Govan & Nelson, 1992) and the difficulty of being eradicated from lung infections due to their intrinsic antibiotic resistance (Nzula *et al.*, 2002). The outcome of CF lung infection by *Bc*c ranges from mild asymptomatic carriage to a rapid and fatal decline in lung function (Isles *et al.*, 1984).

Many studies have been undertaken to understand *Bc*c pathogenicity and several putative virulence factors have been identified (Leitao *et al.*, 2010; Mahenthiralingam *et al.*, 2005). One such factor is the exopolysaccharide (EPS) cepacian produced by a majority of *Bc*c strains (Zlosnik *et al.*, 2008). *In vitro* studies showed the ability of exopolysaccharide to inhibit neutrophil chemotaxis and the production of reactive oxygen species (Bylund *et al.*, 2006). Furthermore, the EPSs produced by a *Burkholderia cenocepacia* clinical isolate interfered with phagocytosis of bacteria by human neutrophils and facilitated bacterial persistent infection in BALB/c mice model of infection (Conway *et al.*, 2004). Using $gp91^{phox-/-}$ mice model of infection, EPS producing strains of *Burkholderia cepacia* were more virulent than nonmucoid isogenic mutants (Sousa *et al.*, 2007). This suggests that EPS enhances bacterial virulence, but

does not rule out that non EPS producers can cause severe infections. That is the case for *B. cenocepacia* and *B. multivorans* isolates, that despite the lack of EPS biosynthesis ability are highly infectious (Govan *et al.*, 1993; Zlosnik *et al.*, 2011). A hypothesis derived from these observations is that mucoid strains would be favored in chronic lung infections while nonmucoid would be more prone to virulence (Zlosnik *et al.*, 2011).

Despite the evidence gained from infection models showing the importance of EPS in *Bc*c virulence, there is no experimental demonstration of *Bc*c bacteria producing it within the lung environment. Contrastingly, in *Pseudomonas aeruginosa*, the major pathogen of the CF lung, the initial colonization is made by environmental strains that during the course of infection develop the mucoid phenotype caused by production of alginate (Pedersen *et al.*, 1992). This mucoid phenotypic conversion was also reported for *Bc*c isolates recovered from CF patients chronically infected, but opposite to *P. aeruginosa*, most transitions were from mucoid to nonmucoid morphotypes (Zlosnik *et al.*, 2008). Characterization of two *B. cenocepacia* sequential isolates displaying different mucoid morphotypes isolated from a CF patient showed differential expression of other phenotypic traits besides EPS (Conway *et al.*, 2004; Zlosnik & Speert, 2010). Contrastingly to *P. aeruginosa* CF lung colonization, where genetic adaptations leading to phenotypic variation are characterized (Smith *et al.*, 2006), the diversity generated by *Burkholderia* persistence in the lungs is mostly unknown. It is therefore of interest to understand trait developments during *Bc*c persistence in CF lungs and to evaluate whether there is a typical phenotypic profile for mucoid and nonmucoid isolates during chronic infections. With that aim, the approach followed was to combine transcriptional profiling using custom *Burkholderia* Affymetrix DNA arrays with phenotypic characterization to compare a

pair of clonal *B. multivorans* sequential isolates recovered from a chronically infected CF patient where a mucoid to nonmucoid morphotypic transition had occurred.

METHODS

Bacterial strains and growth conditions. The *Burkholderia* isolates used are D2095 and D2214 as shown in Table 1. These isolates are from a patient attending a Vancouver CF clinic as previously described (Zlosnik *et al.*, 2008; Zlosnik *et al.*, 2011). Isolates were grown in Lennox broth (LB) or in EPS-producing medium (SM) at 37 °C (Ferreira *et al.*, 2010). Growth under microaerophilic conditions was carried out using microaerophilic generators (GENbox microaer, Biomérieux) contained within a sealed 2 liters jar. For expression profiling, overnight cultures of the isolates were grown in SM medium and were diluted to an initial $OD_{640\ nm}$ of 0.1 into the same medium. Triplicate 250 ml Erlenmeyer flasks containing 100 ml of media were cultured at 37 ºC with 250 r.p.m. agitation for 17 h.

Survival to long-term nutrient deprivation. Liquid cultures of *B. multivorans* D2095 and D2214 grown overnight in LB at 37 ºC, were harvested, washed with saline solution and added to 100 ml M63 minimal medium without a carbon source (Sambrook, 2001), to a final $OD_{640\ nm}$ of 1.0. Cultures were incubated under aerobic conditions for 28 days at 37 ºC with agitation. The number of surviving bacteria was assessed by quantification of colony-forming units (c.f.u.) in LB plates after 48 h incubation at 37 ºC.

Phenotypic assays. (i) Exopolysaccharide production was assessed based on the ethanol-precipitated polysaccharide dry weight recovered from 100 ml bacterial cultures grown in liquid SM over 3 days at 37 ºC, as described before (Ferreira *et al.*, 2007); (ii) Antimicrobial susceptibility tests were based on the agar disc diffusion method (Bauer *et al.*, 1966) against

piperacillin (Pip) (100 µg), piperacillin (75 µg) plus tazobactam (Taz) (10 µg), ciprofloxacin (Cip) (5 µg), ceftazidime (Cef) (30 µg), and amikacin (Ami) (30 µg). The discs were applied onto Mueller-Hinton (Difco Laboratories) agar plates surface previously inoculated with 100 µl of bacterial cultures grown overnight in SM, at 37 °C, and diluted to $OD_{640\ nm}$ of 0.1. Growth inhibition diameter was measured after 24 h of incubation at 37 °C; (iii) For zone inhibition assays, bacteria were grown in SM medium and 100 µl of a culture with $OD_{640\ nm}$ of 1.0 were spread onto SM plates. Sterile paper disks 6 mm in diameter were placed on the agar surface. A total of 20 µl of sodium dodecyl sulphate (SDS) (10 % w/v), sodium deoxycholate (DOC) (5 % w/v), cumene hydroperoxide (CHP) (10 % v/v), and H_2O_2 (30 % v/v) was pipetted onto separate disks. The plates were incubated for 24 h at 37 ºC and zone growth inhibition measured; (iv) Biofilm formation assays were performed as previously described (Ferreira *et al.*, 2007). Bacteria were grown in SM medium at 37 °C until mid-exponential phase, diluted to an $OD_{640\ nm}$ of 0.05 and 200 µl of these cell suspensions were inoculated into wells of a 96-well polystyrene microtiter plate. Plates were incubated at 37 ºC without agitation under normal atmosphere or under microaerophilic conditions inside anaerobic jars. The biofilm was stained with a crystal violet solution, followed by dye solubilization with ethanol and measurement of the solution absorbance at 590 nm using a microplate reader as previously described (Ferreira *et al.*, 2007); (v) Swimming plates with 0.3 % (w/v) Bacto agar (Difco) and swarming plates with 0.5 % (w/v) Noble agar (Difco) were prepared using Broomfield medium (0.04 % tryptone (w/v); 0.01 % yeast extract (w/v); and 0.0067 % (w/v) $CaCl_2$) and LB with 0.5 % (w/v) glucose, respectively. For estimation of motility, overnight SM bacterial cultures (5 µl) were inoculated onto agar surface and incubated at 37 ºC for 48 h followed by colony diameter determination.

Virulence determination in *Galleria mellonella*. Killing assays were performed as previously described (Seed & Dennis, 2008). Larvae were injected with an increasing number of bacteria ranging from $7x10^3$ to $7x10^6$ c.f.u. diluted in 10 mM $MgSO_4$ with 1.2 mg ml^{-1} ampicillin and the survival rate evaluated for 6 days post-infection. As a negative control, 10 mM $MgSO_4$ with 1.2 mg ml^{-1} ampicillin was used. Triplicates of ten larvae were used in each experiment.

Bacterial genotyping. Sample preparation and pulsed-field gel electrophoresis (PFGE) was performed as previously described (Moreira *et al.*, 1997). Prior to PFGE, immobilized DNA was digested with 20 U of *Spe*I restriction endonuclease before being loaded into a 1 % (w/v) agarose gel in 0.5x Tris-borate-EDTA buffer. PFGE was carried out with a Gene Navigator apparatus (Pharmacia-LKB, Sweden) at 180 V, using 5-120 seconds pulse times for 22 h.

recA gene amplification and restriction fragment length polymorphism analysis was performed to confirm that the two isolates belong to *B. multivorans*. The primers used for *recA* amplification were BCR1 (TGACCGCCGAGAAGAGCAA) and BCR2 (CTCTTCTTCGTCCATCGCCTC), followed by *Hae*III digestion of the 1043-bp amplification product.

Custom *Burkholderia* microarray design. Nucleotide sequences used for microarray design were from *B. multivorans* ATCC 17616 and *B. cenocepacia* J2315 genomes present in GenBank. Sequences corresponding to coding regions from the two genomes were aligned against each other based on BLASTN (Altschul *et al.*, 1997). Using the web tools available

through the Personal BLAST Navigator (PLAN) (He *et al.*, 2007) system, genes with >90 % identity at nucleotide level were targeted and exported into tabular format for common probe selection. The parameters chosen for the custom array design were as follows: 11-μm feature size, standard 12.8-mm array format, prokaryotic antisense target type, perfect-match probes only, full length sequence for probe selection, and eight as the minimum acceptable probes per sequence. The types of probe sets represented are: 10,032 unique; 3,342 gene (_a); 247 identical (_s); and 1,203 mixed (_x). *B. cenocepacia* J2315 genes are represented by 4,790 unique probes; 3,210 gene (_a); 136 identical (_s); and 676 mixed (_x). *B. multivorans* ATCC 17616 genes are represented by 5,099 unique probes; 3,268 gene (_a); 158 identical (_s); and 766 mixed (_x). A total of 280 probe sets representing 213 regions of *B. cenocepacia* J2315 genome encoding putative non-coding small RNAs as predicted elsewhere (Coenye *et al.*, 2007) were also included. Probe gene coverage is 99.0 and 99.8 % for *B. cenocepacia* J2315 and *B. multivorans* ATCC 17616, respectively.

Isolation and processing of RNA and DNA samples. For RNA analysis bacterial cells were resuspended in RNAprotect bacteria reagent (Qiagen), and total RNA extraction was carried out using the RNeasy MiniKit (Qiagen) by following manufacturer's recommendation. RNA integrity was checked on an Agilent 2100 Bioanalyser using an RNA Nano assay. RNA was processed for use on Affymetrix custom dual species *Burkholderia* arrays, according to the manufacturer's Prokaryotic Target Preparation Assay. Briefly, 10 μg of total RNA containing spiked in Poly-A RNA controls (GeneChip Poly-A RNA Control Kit; Affymetrix, Santa Clara, CA) was used in a reverse transcription reaction with random primers (Invitrogen Life Technologies) to generate first-strand cDNA. After removal of RNA, 2 μg of cDNA were

197 fragmented with DNase and end-labeled with biotin using terminal polynucleotidyl transferase
198 (GeneChip® WT Terminal Labeling Kit, Affymetrix). Size distribution of the fragmented and
199 end-labeled cDNA was assessed using an Agilent 2100 Bioanalyzer. 2 µg of end-labeled
200 fragmented cDNA were used in a 200-µl hybridization cocktail containing added hybridization
201 controls and hybridized on arrays for 16 h at 50 ºC. Modified post-hybridization wash and
202 double-stain protocols (FLEX450_0005; GeneChip HWS kit, Affymetrix) were used on an
203 Affymetrix GeneChip Fluidics Station 450. Arrays were scanned on an Affymetrix GeneChip
204 scanner 3000 7G. Biological triplicates of RNA from each bacterial culture were processed and
205 analyzed.
206
207 For DNA analysis bacterial cells were grown in liquid LB for 15h, followed by DNA
208 extraction using the DNeasy blood and tissue kit (Qiagen). A total of 1.5 µg of genomic DNA
209 per sample was labeled using the Bioprime DNA labelling System (Invitrogen,Paisley, UK)
210 following a strategy for genomic DNA hybridizations to GeneChips developed by Hammond
211 and co-authors (Hammond *et al.*, 2005). Cleanup was performed using MinElute PCR
212 Purification Kit (Qiagen, Hilden) and quality was checked on an Agilent 2100 Bioanalyser
213 using a DNA 1000 assay. 5 µg per sample were analyzed on Affymetrix custom dual species
214 *Burkholderia* arrays following the protocol described above for RNA samples. Duplicates of
215 DNA from each bacterial culture were processed and analyzed.
216
217 **Microarray analysis.** For RNA analysis scanned arrays were analyzed with Affymetrix
218 Expression Console software to assure that all quality parameters were in the recommended
219 range. Subsequent analysis was carried out with DNA-Chip Analyzer 2008. First a digital

mask was applied, leaving for analysis only the 9291 probe sets representing *B. multivorans* ATCC 17616 transcripts. Then the 6 arrays were normalized to a baseline array with median CEL intensity by applying an Invariant Set Normalization Method (Li & Wong, 2001a). Normalized CEL intensities of the arrays were used to obtain model-based gene expression indices based on a Perfect Match (PM)-only model (Li & Wong, 2001b). Replicate data (triplicates) for each bacterial isolate was weighted gene-wise by using inverse squared standard error as weights. All genes compared were considered to be differentially expressed if the 90 % lower confidence bound of the fold change (LCB) between experiment and baseline was above 1.2, resulting in 392 differentially expressed transcripts with a median False Discovery Rate (FDR) of 4.7 %.

For DNA a separate analysis was performed for the 4 arrays following the steps described above for RNA. An LCB cut-off of 1.5 in combination with a consistent hybridization signal above 10 in the two replicas of at least one strain was chosen, resulting in 52 genomic loci showing significantly different hybridization signals.

Quantitative real-time RT-PCR. DNA microarray data were validated by qRT-PCR as previously described (Ferreira *et al.*, 2010). Total RNA was used in a reverse transcription reaction with TaqMan Reverse Transcription Reagents (Applied Biosystems). qRT-PCR amplification of each gene (for primer sequence see Supplementary Table S1) was performed with a model 7500 thermocycler (Applied Biosystems). The expression ratio of the target genes relative to the reference gene *trpB*, which showed no variation in the transcription

abundance under the conditions tested, was determined. Relative quantification of gene expression by real-time qRT-PCR was determined using the $\Delta\Delta C_t$ method (Pfaffl, 2001).

Microarray data accession number. Microarray data were deposited in the Gene Expression Omnibus (GEO) repository at NCBI under accession numbers: GSE28306 (for expression data) and GSE30402 (for genomic DNA hybridization).

RESULTS

Mucoid phenotype assessment in sequential isolates of *B. multivorans*

Within a 13-year period 12 isolates were recovered from a cystic fibrosis patient persistently infected with *Burkholderia* (Table 1). This patient, which is still alive, had simultaneously cultured other bacteria such as *Staphylococcus aureus* and *Pseudomonas aeruginosa*, but at the time of the last six isolates only *B. multivorans* was present. These isolates were analyzed by randomly amplified polymorphic DNA (RAPD) and all of them belonged to RAPD group BM-019, corresponding to the same *B. multivorans* strain (Zlosnik *et al.*, 2008). The assessment of exopolysaccharide production in yeast extract mannitol (YEM) agar showed that isolates recovered from November 1993 until June 2006 were mucoid although some variation in the amount of EPS was observed (Table 1). Interestingly, the last isolate (D2214) was completely nonmucoid and represents a mucoid to nonmucoid transition. Additional confirmation that mucoid D2095 and nonmucoid D2214 are indeed clonal came from pulsed-field gel electrophoresis of genomic DNA digested with *Spe*I restriction endonuclease, since the DNA fragments pattern obtained is almost identical (Fig. S1). Specific primers to amplify the *recA* gene from *Burkholderia* followed by restriction analysis with *Hae*III also confirmed that both isolates are indeed from the species *B. multivorans* (data not shown).

Isolates D2095 and D2214 were chosen here to gain insights into phenotypic variation during *Bcc* chronic lung infection and in particular to assess differences between the mucoid and nonmucoid morphotypes. Two of the analyzed features were growth behavior under aerobic

conditions and production of exopolysaccharide in SM liquid medium. Both isolates displayed identical growth rates (Fig. 1a), but EPS biosynthesis results confirmed that D2095 produces approximately 10 g l^{-1} after 72 h of growth, while from the supernatant of D2214 no EPS was recovered (Fig. 1b), confirming the morphotypes obtained previously in YEM (Zlosnik *et al.*, 2008).

Expression profiling among sequential *B. multivorans* mucoid and nonmucoid isolates

To understand the differences between isolates D2095 and D2214, transcriptional profiling was performed and data mapped to cellular processes and metabolic pathways. For that, a dual species custom *Burkholderia* microarray (Bcc1sa520656F) was designed and produced by Affymetrix as described in the Methods section. One of species represented in the array is *B. multivorans* ATCC 17616 and its coding regions are represented by 5,099 unique probes; 3,268 gene (_a); 158 identical (_s); and 766 mixed (_x) with gene coverage of 99.8 %. To determine which probes from the array hybridize differentially between the genomes of *B. multivorans* D2095 and D2214, both genomic DNAs were extracted, biotin-labeled and hybridized in duplicate to the microarray Bcc1sa520656F. Genomic DNA hybridization intensities from D2214 were compared to the ones of D2095 using dChip (≥ 1.5-fold change lower confidence bound and hybridization signal above 10), resulting in 52 genes with differential hybridization (Supplementary Table S2). The majority of these genes are located very close to each other on chromosome 2. Genes Bmul_4779 up to Bmul_4788 seem to be absent from D2214 isolate genome as shown by the image of the probe-set intensities in both isolates for gene Bmul_4779 (Fig. S2a). These genes encode putative ABC transporter related

proteins and a transcriptional regulator of the MarR family. Another region most likely absent from D2214 comprises genes Bmul_4804 up to Bmul_4812 with the exception of Bmul_4807, putatively involved in the degradation pathway of phthalate. Finally, the largest group of genes comprising Bmul_4834 up to Bmul_4874 (with a few exceptions), seem to be duplicated in D2214 genome. Since the probe-sets corresponding to these genes showed hybridization signals (for an example see Fig. S2b), it is unlike that it corresponds to a deletion in D2095 genome. All these last group of genes encode proteins putatively related to bacteriophages. From this genomic hybridization experiment we demonstrate that indeed some genetic alterations took place during lung colonization by these isolates.

To carry out transcription profiling, RNA was extracted from the mucoid D2095 and the nonmucoid D2214 isolates grown in SM medium until early stationary phase, corresponding to a period where high molecular weight EPS is not yet recovered from the culture supernatant. The expression profile of D2214 when compared to D2095 using dChip ($\geq$ 1.2-fold change lower confidence bound with a resulting FDR of $\leq$4.7%) showed 113 genes with significantly increased expression (Supplementary Table S3) and 279 genes with significantly decreased expression (Supplementary Table S4). The search for common genes between the expression data and the genomic hybridization data showed 22 genes, 8 increased in both data sets and 14 decreased (Fig. 2). These genes were excluded from our expression analysis, leaving us with 105 genes with significantly increased expression and 265 with significantly decreased expression (Fig. 2). Clusters of Orthologous Groups (COGs) were attributed to the differentially expressed genes as shown in Fig. 3. No particular categories with a high number of genes with significantly increased expression were obtained (Fig. 3, grey bars). Categories

with a high number of genes with significantly decreased expression were cell wall/membrane/envelope biogenesis and cell motility (Fig. 3, black bars). There was no preferential distribution of differentially expressed genes within the three replicons, with 6.8, 6.8, and 3.5 % of the genes from chromosome 1, 2 and 3, respectively, being differentially expressed.

To confirm data obtained by microarray analysis, expression of 7 representative genes from COGs K, M, N and T was analyzed by qRT-PCR. Results obtained were in good agreement with microarray data although the fold change for most of the genes was higher when expression was analyzed by qRT-PCR (Table 2).

Genes involved in virulence traits

In general, a decrease in transcripts of genes encoding virulence-associated traits, such as motility, chemotaxis, type-VI secretion, antibiotic resistance, among others was observed in D2214 (Table 3 and Supplementary Table S4). Concerning motility and chemotaxis, all *flh*, *flg*, *mot*, *fli* and *che* gene-encoding products showed a decreased expression in D2214 when compared to D2095 (Table 3). The sole exceptions were the filament encoding genes *fliCD* and *fliOPQR* whose gene products are involved in flagella assembly, with no significant change. Besides the decreased expression of several genes encoding methyl-accepting chemotaxis proteins, D2214 isolate also displayed a decreased expression of the *aer* gene encoding a protein homologous to the aerotaxis (oxygen-sensing) receptor Aer from other bacteria. Through control of the flagellar motor Aer sensing enables motile bacteria to avoid niches

where carbon deficiency, hypoxia or other insults would limit energy production (Taylor, 2007). To confirm the microarray data, swimming and swarming motilities were assessed by quantitative plate assays. Under the conditions tested, D2214 showed a reduction of 15% of swimming motility and 45% of swarming motility when the size of the colonies formed were compared with the ones of the D2095 isolate (Fig. 4a).

Another set of genes with significantly decreased expression in isolate D2214 were the ones encoding products required for type-VI secretion. In fact, 9 out of the 18 genes annotated as involved in type-VI secretion showed differential expression (Table 3). Although type-VI encoding genes are poorly expressed under *in vitro* laboratory conditions, this type of transport was discovered as a novel factor of *B. cenocepacia* survival in a rat model of chronic lung infection (Aubert *et al.*, 2010; Hunt *et al.*, 2004). In a recent study, Schwarz and co-authors proposed a broader physiological significance of type-VI secretion to provide defense against simple eukaryotic cells and other bacteria in the environment (Schwarz *et al.*, 2010). Co-inoculation of D2095 and D2214 isolates in SM liquid medium for three days at 37 ºC followed by mucoid *vs* nonmucoid c.f.u. determination indicated that none of the strains predominate over the other (data not shown). As control, single cultures were grown under the same tested conditions to demonstrate that no morphotype variation occurred during that period of time.

The expression of genes Bmul_1515 and Bmul_6008, encoding two putative beta-lactamases, was significantly decreased in D2214 isolate (Table 3). This was consistent with the intrinsic antibiotic resistance pattern obtained by using the antibiotic disc assay. The inhibition halos

obtained in the presence of ciprofloxacin, ceftazidime and amikacin were very similar for both isolates, but for the beta-lactam piperacillin alone or with tazobactam, isolate D2095 was significantly more resistant than D2214 (Fig. 4b). The same result was obtained in liquid cultures supplemented with each of the antibiotics under test (data not shown).

Other genes encoding putative virulence factors which had a decreased expression in D2214 were Bmul_3709, Bmul_3710 and Bmul_3712, directing the synthesis of a hemolysin-type calcium-binding protein and a type-I transporter from the HlyD family (Table 3); and the acid phosphatase encoding gene Bmul_4180. The protein encoded by Bmul_4180 is homologous to AcpA from *B. pseudomallei* and, although being considered a putative virulence factor, the disruption of the *acpA* gene from *B. pseudomallei* did not significantly reduce the virulence of this organism (Burtnick *et al.*, 2001).

Bcc bacteria are most probably subjected to oxidative stress in the lung, as caused by the enormous presence of neutrophils (Downey *et al.*, 2009). Although none of the genes usually found as involved in combating oxidative stress were differentially expressed in our data set, the behavior of both isolates under this type of stress was evaluated. We have compared the resistance of D2095 and D2214 isolates grown in the presence of cumene hydroperoxide (CHP) and H_2O_2 (Fig. 4c) with the results confirming that isolates react with the same magnitude to oxidative stress. Stress induced by SDS and DOC was also tested and the results showed a slight increase in susceptibility by D2214 (Fig. 4c).

Biofilm formation contributes to infection by protecting the bacteria from the host immune defence (Costerton *et al.,* 1999). To assess biofilm formation in an abiotic surface by D2095 and D2214, a quantitative assay using crystal violet was used. After 48 h of incubation under aerophilic conditions, the adherence level by isolate D2214 was slightly bigger than the one of D2095, as visible by the optical density of the solubilized dye (Fig. 5a). Interestingly, when the biofilm was formed under microaerophilic conditions, this difference became much more prominent, suggesting that a reduction of the oxygen level favored D2214 biofilm formation (Fig. 5a).

Galleria mellonella was used as an acute model of infection to compare the virulence of the mucoid D2095 and nonmucoid D2214 isolate. Several inoculums ranging from $7x10^3$ up to $7x10^6$ c.f.u. were used for both isolates. For the lower number of bacteria (approximately $7x10^3$ and $7x10^4$ c.f.u.), none of the larvae was dead after 6 days post-infection (data not shown). When approximately $7x10^5$ c.f.u. were used it was observed virulence attenuation by nonmucoid D2214, with more than 80% of the larvae still being alive after 4 days post-infection while in D2095 only 10% remained alive (Fig. 5b, open symbols). A larger inoculum size (approximately $7x10^6$ c.f.u.) also showed virulence attenuation for D2214 when compared to D2095, but in this case larvae survival rate was less pronounced in the presence of both isolates (Fig. 5b, filled symbols). These data showing higher survival rate in the presence of D2214 confirm the decreased expression of many transcripts encoding proteins putatively involved in virulence that we observed in our microarray data. Nevertheless, for prolonged incubation time and a large inoculum size, both strains display a fully virulent phenotype.

Genes involved in cell wall

In the category of cell wall biogenesis, the largest group of genes differentially expressed comprises the *bce* genes involved in cepacian biosynthesis (Table 3). All genes from both *bce-I* and *bce-II* gene clusters (Ferreira *et al.*, 2010; Moreira *et al.*, 2003) showed strong decreased expression in D2214 in comparison to D2095. In fact, 15 out of 19 genes had more than 2-fold decreased expression. This result partially confirms the nonmucoid phenotype observed for D2214 and suggests that regulation of cepacian biosynthesis in this isolate is probably at the transcriptional level, but post-transcriptional regulation may also account for that.

Some differences at the outer membrane composition of the two isolates may also be present since many genes encoding outer membrane porins showed a decreased expression in D2214. These genes are *ompW*, Bmul_0880, Bmul_2395, Bmul_2847, Bmul_3710 and Bmul_4600. The decrease in the expression levels for porin encoding genes could indicate a less permeable outer membrane in this isolate.

Genes involved in transcription and signal transduction

In the category of transcriptional regulators, the expression of five genes encoding products involved in motility and chemotaxis regulation was found as being decreased in D2214 (Table 3). These genes encode the master regulators FlhCD, the sigma 28 subunit of RNA polymerase FliA, the anti-sigma 28 FlgM and CheY protein, which when phosphorylated binds to FliM

and changes flagellar motor rotation. As described before, most of the genes under control of these regulators showed decreased expression in D2214.

Genes Bmul_4264 and Bmul_4265, encoding a response regulator receiver protein and a transcriptional regulator of the Crp/Fnr family, respectively, showed a decreased expression in D2214 isolate (Table 3). The Crp (cAMP receptor protein)-like and Fnr (fumarate and nitrate reductase regulatory protein)-like transcription factors comprise proteins which respond directly or indirectly to a broad spectrum of intracellular and exogenous signals (cAMP, oxygen or redox state, oxidative and nitrosative stress, nitric oxide, carbon monoxide, 2-oxoglutarate or temperature) (Korner *et al.,* 2003). Dufour and co-authors analyzed the Crp/Fnr conserved regulons within α-proteobacteria and found that the core Fnr regulon encodes enzymes for microaerobic or anaerobic respiratory growth, including synthesis of heme, the high-affinity cytochrome *cbb3*-type oxidase, metal cation transporters, the OmpW porin, the universal stress protein UspA, among others (Dufour *et al.*, 2010). To our knowledge none of the *Burkholderia* Crp/Fnr regulators has been characterized, but it is interesting to observe that genes Bmul_2345 encoding a heavy metal translocating P-type ATPase; Bmul_5381 encoding a UspA protein; Bmul_0982 encoding a coproporphyrinogen oxidase; gene *ompW* and the *narGHIJ* genes encoding nitrate reductase, all showed a decreased expression in D2214. The decreased expression of gene-encoding products such as the FNR-type regulator and nitrate reductase in D2214 suggests that this isolate is less adapted to survive under low oxygen tension. To test this hypothesis, isolates D2095 and D2214 were grown in SM medium at 37ºC under microaerophilic conditions. Growth curves shown in Fig. 1a confirmed the slower

growth rate and lower biomass formed by D2214 when compared to D2095 during the 48 hours of growth.

Genes involved in energy and central intermediary metabolism

We found decreased expression of several genes involved in central metabolism and energy production in D2214, suggesting lower energetic needs of this isolate. For instance, a decrease of the expression of some *smoEFGK* genes involved in the uptake of mannitol, the carbon source provided in our experiment, was observed. Similarly, gene *mtlK*, encoding a mannitol dehydrogenase enzyme converting D-mannitol into D-fructose and the fructokinase encoding gene Bmul_0700 converting D-fructose into D-fructose-6P showed decreased expression in D2214 (Table 3). Another set of genes encoding a putative monosaccharide transporter encoded by Bmul_3783 to Bmul_3785 (Table 3) showed a decreased expression in D2214, reinforcing the idea of reduced sugar uptake needs.

Concerning other carbohydrate metabolism reactions, a decrease in expression of many genes encoding enzymes leading to the cepacian nucleotide sugar precursors was observed. Besides decreased expression of *bceACMNT*, the expression of genes Bmul_2501 and Bmul_2506 encoding putative UDP-glucose epimerases converting UDP-glucose into UDP-galactose was decreased in D2214. A set of genes with increased expression in D2214 are putatively involved in osmotic stress response and encode an ABC-transporter (Bmul_3511 and Bmul_3512) and a protein putatively involved in the synthesis of the osmo-protectant α-trehalose (gene *otsA*) (Table 3). Regarding energy production and conversion, three genes (Bmul_1434 to

476 Bmul_1436) encoding products involved in the formation of acetyl-CoA from pyruvate,
477 showed a decreased expression in D2214 (Table 3). That may indicate a lower availability of
478 acetyl-CoA for the TCA cycle and consequently a reduction of anabolic pathways and ATP
479 synthesis.
480
481 Many genes involved in nitrogen metabolism had decreased expression in D2214. That is the
482 case for a cluster of six genes probably involved in anaerobic nitrate respiration. Those genes
483 seem to be an operonic structure composed of *narGHJI* encoding nitrate reductase, gene
484 Bmul_5387 encoding a peptidyl-prolyl cis-trans isomerase and *narK* encoding a nitrate/nitrite
485 antiporter. Since gene expression was measured under aerobic conditions, the decreased
486 expression of genes involved in nitrate respiration may suggest that D2214 has a tighter control
487 on the expression of genes whose products are not necessary for bacterial survival, but may
488 also reflect the lower ability to survive under low oxygen as we have shown. Other genes
489 involved in nitrogen metabolism with decreased expression are required for glutamate
490 biosynthesis, a central metabolite providing nitrogen for the synthesis of all other N-containing
491 components. These were the GOGAT encoding genes *gltBD* as well as glutamate
492 dehydrogenase *gdhA*. Although not to a great extent, the differential expression of genes
493 encoding enzymes for amino acid biosynthesis was primarily decreased in D2214. Decreased
494 expression in D2214 of Bmul_1255 encoding the primary nitrogen sensor GlnD was also
495 observed (Table 3). D2214 probably senses an excess of nitrogen, and therefore many genes
496 related to its metabolism have a decreased expression. Together, these results may reflect the
497 lower need of nitrogen and carbon compounds by D2214. This may mirror the lack of EPS

biosynthesis burden, although cells were collected several hours before high molecular weight EPS was detected in the supernatant, or is a broader adaptation mechanism to save energy.

To evaluate whether the metabolic differences observed at the transcriptional level between D2095 and D2214 could give rise to different survival ability, both cultures were aerobically incubated for a prolonged period of time (28 days) under nutrient starvation in minimal medium without a carbon source. Colony-forming units (c.f.u.) counting showed higher survival rate of D2214 over the full incubation period (Fig. 6).

DISCUSSION

One of the conclusions derived from our analysis is the confirmation that during the course of chronic lung colonization by *Burkholderia*, genetic or epigenetic changes leading to development of new bacterial phenotypes arise. These different phenotypes are much more than just mucoid variation and have repercussions in other virulence traits and metabolism. The combined analysis of transcriptional profiling and phenotypic assays allowed us to observe a general reduction of the expression of several virulence factors in the nonmucoid D2214 isolate when compared with the clonal mucoid isolate D2095. This was observed for swimming and swarming motility, type-VI secretion, hemolysin-type protein secretion and exopolysaccharide production. To evaluate whether these changes had an effect on *Burkholderia* virulence, we had chosen *G. mellonella* as an animal model for acute infection assessment (Seed & Dennis, 2008). The results here presented showed that D2214 isolate displayed reduced acute virulence when compared to D2095, but it was still able to kill approximately 90% of the larvae within the time period of the experiment and for the highest cell density tested. Another phenotype displayed by D2214 was a decrease in resistance to some β-lactam antibiotics. This is an unusual result since due to the antibiotic therapies administered to CF patients, bacteria tend to develop higher resistance. The lower resistance level of D2214 isolate against some β-lactam antibiotics may be due to pleiotropic effects of the mutation(s) occurred in this isolate and is most likely not relevant clinically. Isolate D2214 forms a biofilm with more biomass than D2095 and, despite a lower growth rate under microaerophilic conditions, this effect is more pronounced under this low oxygen tension. This result of biofilm formation ability is in accordance with the lower motility and chemotactic

responses displayed by D2214 and may indicate a preference of this bacterium to live under a sessile lifestyle, especially if areas of low oxygen tension are available within the lungs and/or chemotactic gradients of nutrients are absent. Similarly, biofilm formation by the nonmucoid *B. cenocepacia* C8963 isolate was shown to be higher than in the highly mucoid C9343, both sequential isolates from a CF patient (Conway *et al.*, 2004). Nevertheless, our result was unexpected due to previous studies showing the positive effect on biofilm formation by the presence of exopolysaccharide production in *B. cepacia* IST408 CF isolate (Cunha *et al.*, 2004; Ferreira *et al.*, 2007). It is then possible that in D2214, especially under microaerophilic conditions, other determinants of biofilm formation may become relevant.

When growing aerobically in rich medium, D2095 and D2214 showed a similar growth rate. In addition, no significant differences in metabolizing 95 sources of carbon and nitrogen present on Microlog GN2 panels were detected for the two isolates (data not shown). Nevertheless, expression data from cells growing under the same conditions showed a decreased expression in many genes involved in carbon and nitrogen metabolism in D2214 isolate. This shutdown of unnecessary transcripts and proteins may reflect lower energetic needs since not so much energy has to be expended on motility and polysaccharide production, two very energetically demanding processes. It is also possible that the decreased expression of many genes involved in metabolism is an adaptation to thrive in an environment, such as the CF lung, where the availability of nutrients varies and other bacterial competitors are present. That could explain the improved survival of D2214 under nutrient starvation for a prolonged period of time.

552 The first pair of sequential isolates of *B. cenocepacia* that have been characterized were
553 recovered within 10 months of each other from a chronically infected CF patient (Conway *et*
554 *al.*, 2004; Zlosnik & Speert, 2010). The earliest isolate, C8963, was nonmucoid and the latest,
555 C9343, was very mucoid. The comparison of C8963 isolate with C9343 by PFGE showed
556 several *Spe*I-digested chromosomal fragments of a different size (Conway *et al.*, 2004) and
557 C9343 had mutations in the quorum sensing regulator encoding gene *cepR* and deletion of a
558 region from the pathogenicity island present mostly in *B. cenocepacia* (McKeon *et al.*, 2011;
559 Zlosnik & Speert, 2010). Our data from the differential genomic DNA hybridization of D2095
560 and D2214 against *B. multivorans* ATCC 17616 genome also demonstrated genetic variation
561 within a region of chromosome 2, resulting in deletion and duplication of genes, confirming
562 that genotypic variation occurs during the course of chronic infection by bacteria. Results from
563 transcriptomic and proteomic analyses in those *B. cenocepacia* isolates showed that the
564 nonmucoid isolate, C8963, had increased expression of virulence factors such as the
565 nematocidal protein AidA or the zinc metalloprotease ZmpA, and was more resistant to
566 oxidative stress (Zlosnik & Speert, 2010). The genes and proteins with lower expression in
567 C8963 were related to metabolism and transport (Zlosnik & Speert, 2010). In addition,
568 nonmucoid C8963 was binding more efficiently to cells of the immune system and displayed a
569 higher clearance rate from the lungs of BALB/c mice when compared to mucoid C9343 isolate
570 (Conway *et al.*, 2004). In our pair of *B. multivorans* D2095/D2214 isolates we observed the
571 same general decreased expression of genes involved in metabolism and transport functions,
572 but also a clear shutdown of the expression of some genes involved in virulence traits. This
573 probably explains the slower mortality rate that we observed for *G. mellonella*. Since two

574 different infection models were used to assess C8963/C9343 (Conway *et al.*, 2004) and
575 D2095/D2214 virulence, it is not possible to compare the results obtained in both cases.
576
577 Considering the mucoid phenotype displayed by isolates *B. multivorans* C5568 up to D2095, it
578 is likely that during the 13-years of lung colonization some fitness-improving mutations may
579 have occurred in these bacterial genomes, although they did not impair bacteria from being
580 able to produce EPS. Contrastingly, in isolate D2214, additional changes must have occurred
581 so that not only polysaccharide production ability was suppressed but many other phenotypic
582 traits also showed considerable variation. What does this mean in terms of bacterial fitness to
583 persist in the CF lung? Considering that the main characteristics of the CF lung environment
584 are the host immune system, antibiotic therapies and substrate composition, the D2214 isolate,
585 by its ability to decrease the expression of several virulence traits and perhaps better escape
586 from the immune system, to form more biofilm, and a better management of nutrient resources,
587 may have increased fitness under all those circumstances. These findings are in agreement with
588 the observed inverse correlation between the ability of *Bc*c bacteria to produce EPS and decline
589 rate of CF lung function (Zlosnik *et al.*, 2011). Nevertheless, other pairs of mucoid/nonmucoid
590 clonal isolates from other *Bc*c species should be tested to evaluate the possibly increased
591 fitness of the nonmucoid variants.
592
593 Data obtained from the transcriptional analysis do not allow us to suggest any specific
594 mechanism behind the morphotype variation observed between D2095 and D2214. It could
595 consist either of the additive effects of several mutations, or by a mutation in a particular
596 regulatory gene with profound pleiotropic effects. Since hypermutable strains of *P. aeruginosa*

are common in persistently infected CF patients (Oliver *et al.*, 2000), we sequenced the *mutS* and *mutL* genes involved in DNA mismatch repair of D2095 and D2214, but no nucleotide differences were found. Therefore, full DNA sequence determination of both genomes is required. Some other mechanisms responsible for genotypic and phenotypic variation within CF isolates of *P. aeruginosa* obtained from colonized lungs are well known (Huse *et al.*, 2010; Smith *et al.*, 2006). Genome sequence determination of two *P. aeruginosa* isolates from one CF patient, recovered with a time offset of 90 months, showed several mutations in regulators and virulence factors in the last isolate, including O-antigen biosynthesis, type-III secretion, motility, multidrug efflux, osmotic balance, phenazine biosynthesis, quorum sensing and iron acquisition (Smith *et al.*, 2006). Analysis of such mutations in a vast collection of isolates showed that the most frequently mutated genes were *mexZ*, a negative regulator of an efflux pump, and *lasR*, the primary regulator of quorum sensing (Smith *et al.*, 2006). Another mutation that has stronger implications in disease progression is in the regulatory gene *mucA* that increases alginate production (Martin *et al.*, 1993; Rau *et al.*, 2010). No protein homologue to anti-sigma factor MucA can be found in *Burkholderia* genomes and the player(s) directly regulating EPS production in these microorganisms remain unknown. Although the differences at the genetic or epigenetic level giving rise to phenotypic variability in CF isolates are not yet known, our results point to some mechanisms used by *Bc*c bacteria for persistence in the lung and will hopefully help to identify vulnerabilities and potential targets for future antimicrobial agent development against these microorganisms.

618 **ACKNOWLEDGMENTS**

619

620 This work was supported by FEDER and Fundação para a Ciência e a Tecnologia, Portugal
621 (contract PTDC/BIA-MIC/66977/2006, a Post-doctoral grant to A.S.F. and doctoral grants to
622 I.N.S. and D.M-H.).

623

LEGENDS

Fig. 1. Growth curves (a) and exopolysaccharide production (b) by *B. multivorans* D2095 under aerobic (□) or microaerophilic (■) conditions and D2214 under aerobic (♦) or microaerophilic (◊) conditions grown in SM medium at 37 ºC. The standard deviation (SD) in both panels is below 5 %. The data are based on mean values from the results of at least three independent cell cultivations.

Fig. 2. Diagram representing the intersection between the differentially expressed genes and the genomic DNA differential hybridization when D2214 was compared with D2095. Genes excluded from our expression data set are indicated.

Fig. 3. Functional distribution into COGs of genes with altered expression when the nonmucoid *B. multivorans* D2214 isolate was compared with the mucoid isolate D2095. A total of 370 genes with a statistically significant altered expression were obtained by using a custom Affymetrix *Burkholderia* GeneChip.

Fig. 4. Phenotypic properties displayed by isolates D2095 and D2214. a) Swimming and swarming motilities assayed in 0.3 % or 0.5 % agar plates spotted with 5 µl bacterial cultures incubated at 37 ºC for 48 h, followed by colony diameter estimation; b) Susceptibility to antibiotics determined at 37 ºC after 24 h incubation by measuring the diameter of cell growth inhibition; c) Sensitivity of isolates to stress inducing agents such as 10 % SDS, 5 % DOC, 10 % CHP and 30 % H_2O_2 were determined by measuring growth inhibition halos, after

incubation of plates at 37 ºC for 24 h. The data are based on mean values from the results of at least three independent cell cultivations. Error bars show SD. T-test was performed using GraphPad Prism 5.0 software. A *P* value of < 0.013 was considered significant compared to D2095 (*).

Fig. 5. Comparison between *B. multivorans* D2095 and D2214 isolates relative to: a) biofilm formation and b) virulence in *Galleria mellonella*. The biomass of the biofilm was assessed after 48 h of incubation at 37 ºC in aerophilic and microaerophilic conditions in polystyrene microtiter plates containing SM medium. Virulence tests were performed by injecting *G. mellonella* with *B. multivorans* D2095 using approximately $7x10^5$ (□) and $7x10^6$ (■) cells or *B. multivorans* D2214 with approximately $7x10^5$ (◊) and $7x10^6$ (♦) cells and estimation of larvae survival rates during 6 days. The control experiment without bacteria is also shown (Δ). The data are based on mean values from the results of at least three independent experiments. Error bars show SD. A *P* value of < 0.01 was considered significant compared to D2095 (*).

Fig. 6. Ability of *B. multivorans* D2095 and D2214 isolates to survive starvation on M63 minimal medium without a carbon source. Survival was assessed by c.f.u. determination in LB agar incubated at 37 ºC for 48 h under aerobic conditions. Error bars indicate SD. A *P* value of < 0.034 was considered significant compared to D2095 (*).

Table 1. Mucoid phenotype displayed by *Burkholderia multivorans* sequential isolates recovered from a cystic fibrosis patient chronically infected.

670 **Table 2.** Quantitative real-time RT-PCR analysis performed in *B. multivorans* D2095 and
671 D2214 cells.
672
673 **Table 3.** Selection of a set of differentially expressed genes when *B. multivorans* D2214
674 transcriptome was compared with the one of D2095, separated by functional groups.
675

Table 1.

Isolate	Date of isolation	Source	EPS score*
C5568	30 November 1993	Sputum	+++
C6558	26 May 1995	Throat swab	++
C7148	14 June 1996	Sputum	+++
C7149	14 June 1996	Sputum	++
C7637	06 June 1997	Sputum	+
C8179	20 June 1998	Sputum	++
C9326	23 September 2000	Sputum	++
D0089	29 March 2002	Throat swab	++
D1782	03 October 2005	Throat swab	+++
D2094	01 June 2006	Throat swab	+++
D2095	01 June 2006	Throat swab	+++
D2214	09 November 2006	Sputum	–

* Classification according to Zlosnik and co-authors (Zlosnik *et al.*, 2008): very mucoid isolates are scored with ++ or +++; slightly mucoid are scored with +; nonmucoid isolates are score by –.

681 **Table 2.**

Gene	Microarray lower bound of fold change	Real-time fold change ± SD
Bmul_0161 (*flhC*)	-2.2	-3.5 ± 1.6
Bmul_0195 (*rlpA*)	1.8	1.2 ± 0.1
Bmul_3013 (*flgI*)	-2.3	-3.3 ± 0.2
Bmul_4264	-1.5	-3.1 ± 0.5
Bmul_4265	-1.5	-3.5 ± 1.2
Bmul_4613 (*bceM*)	-3.4	-6.2 ± 1.3
Bmul_4914 (*bceG*)	-18.3	-8.8 ± 0.1

682

683

684 **Table 3.**

Functional class	**Gene identifier**	**LB-FC[1]**	**Gene name**	**Description**
Flagellar	Bmul_0043	**-1.8**	*fliM*	Flagellar motor switch protein FliM
synthesis,	Bmul_0165	**-1.9**	*cheA*	CheA signal transduction histidine kinase
motility and	Bmul_0168	**-1.8**	*cheR*	MCP methyltransferase, CheR-type
chemotaxis*	Bmul_0169	**-2.1**	*cheD*	CheD
	Bmul_0177	**-1.8**	*flhF*	GTP-binding signal recognition particle SRP54 G- domain
	Bmul_0178	**-1.9**	*flhG*	Flagellar biosynthesis protein, FlhG
	Bmul_3010	**-1.9**	*flgK*	Flagellar hook-associated protein FlgK
	Bmul_3013	**-2.3**	*flgI*	Flagellar basal body P-ring protein
	Bmul_3014	**-1.9**	*flgH*	Flagellar basal body L-ring protein
	Bmul_3015	**-1.9**	*flgG*	Flagellar basal-body rod protein FlgG
	Bmul_3018	**-1.9**	*flgD*	Flagellar hook capping protein
	Bmul_3020	**-1.7**	*flgB*	Flagellar basal-body rod protein FlgB
	Bmul_3023	**-2.0**	*flgN*	FlgN family protein
	Bmul_3059	**-1.8**	*fliS*	Flagellar protein FliS
	Bmul_3061	**-1.9**	*fliF*	Flagellar M-ring protein FliF
	Bmul_3062	**-1.9**	*fliG*	Flagellar motor switch protein FliG
	Bmul_3362	**-1.7**	*aer*	Methyl-accepting chemotaxis sensory transducer
Virulence and	Bmul_1515	**-2.2**	-	Beta-lactamase domain protein
pathogenesis	Bmul_2854	**-1.3**	*paaI*	Phenylacetic acid degradation protein PaaD
	Bmul_2923	**-1.3**	*bcsE*	Type VI secretion-associated protein, ImpA family
	Bmul_2924	**-1.3**	*bcsF*	Type VI secretion ATPase, ClpV1 family
	Bmul_2925	**-1.4**	*bcsG*	Type VI secretion protein, VC_A0111 family
	Bmul_2927	**-1.6**	*bcsI*	Type VI secretion system lysozyme-related protein

	Bmul_2928	**-1.3**	*bcsJ*	Type VI secretion system effector, Hcp1 family
	Bmul_2929	**-1.4**	*bcsK*	Type VI secretion protein, EvpB/VC_A0108 family
	Bmul_2930	**-1.3**	*bcsL*	Type VI secretion protein
	Bmul_2931	**-1.3**	*bcsM*	TPR repeat-containing protein
	Bmul_2934	**-1.2**	*bcsP*	Hypothetical protein (type VI)
	Bmul_3709	**-1.3**	*adh*	Hemolysin-type calcium-binding region
	Bmul_3710	**-1.7**	-	Outer membrane efflux protein
	Bmul_3712	**-1.2**	-	Type I secretion membrane fusion protein, HlyD family
	Bmul_6008	**-1.4**	*ampC*	Beta-lactamase
Cell wall/	Bmul_0303	**-1.4**	*ompW*	OmpW family protein
membrane **	Bmul_4605	**-10.2**	*bceT*	UTP-glucose-1-phosphate uridylyltransferase
	Bmul_4612	**-6.3**	*bceN*	GDP-mannose 4,6-dehydratase
	Bmul_4913	**-8.2**	*bceH*	Glycosyltransferase-like protein
	Bmul_4914	**-18.3**	*bceG*	Glycosyl transferase family 2
	Bmul_4915	**-8.1**	*bceF*	Phosphotyrosine autokinase
	Bmul_4916	**-8.4**	*bceE*	Polysaccharide biosynthesis protein
	Bmul_4918	**-10.1**	*bceC*	Nucleotide sugar dehydrogenase
	Bmul_4919	**-4.2**	*bceB*	Undecaprenyl-phosphate glucose phosphotransferase
	Bmul_4920	**-8.0**	*bceA*	Mannose-1P guanylyltransferase/mannose-6P isomerase
Transcription	Bmul_0179	**-1.9**	*fliA*	RNA polymerase, sigma 28 subunit, FliA/WhiG
regulators	Bmul_2557	**-2.1**	-	Transcriptional regulator, LysR family
	Bmul_3022	**-1.7**	*flgM*	Anti-sigma-28 factor, FlgM
	Bmul_3720	**2.9**	-	Transcriptional regulator, XRE family
	Bmul_3782	**-1.8**	-	Transcriptional regulator, AraC family
Regulatory/	Bmul_0160	**-1.5**	*flhD*	Flagellar transcriptional activator

Signal	Bmul_0161	**-2.2**	*flhC*	Flagellar transcriptional activator FlhC
transduction	Bmul_0171	**-1.7**	*cheY*	Response regulator receiver protein
	Bmul_2116	**-1.5**	-	Diguanylate cyclase/phosphodiesterase with PAS/PAC sensor
	Bmul_3168	**-1.5**	-	Response regulator receiver protein
	Bmul_4264	**-1.5**	-	Response regulator receiver protein
	Bmul_4265	**-1.5**	*Fnr*	Transcriptional regulator, Crp/Fnr family
	Bmul_5122	**-1.2**	-	Diguanylate cyclase/phosphodiesterase with PAS/PAC sensor
Energy	Bmul_1434	**-2.1**	*pdhA*	Dehydrogenase E1 component
production	Bmul_1435	**-1.7**	*pdhB*	Transketolase central region
and	Bmul_1436	**-1.3**	_	Branched-chain alpha-keto acid dehydrogenase subunit E2
conversion	Bmul_2651	**-1.7**	*dld*	FAD linked oxidase domain protein (lactate dehydrogenase)
	Bmul_2652	**-1.6**	*glcD*	FAD linked oxidase domain protein (glycolate oxidase)
	Bmul_5383	**-1.5**	*narG*	Nitrate reductase, alpha subunit
	Bmul_5384	**-1.4**	*narH*	Nitrate reductase, beta subunit
	Bmul_5385	**-1.7**	*narJ*	Nitrate reductase molybdenum cofactor assembly chaperone
	Bmul_5386	**-1.3**	*narI*	Respiratory nitrate reductase, gamma subunit
	Bmul_5388	**-1.3**	*narK*	Major facilitator superfamily MFS_1
Carbohydrate	Bmul_0700	**-1.3**	-	Pfkb domain protein
transport and	Bmul_0702	**-1.5**	*smoE*	Extracellular solute binding protein
metabolism	Bmul_0706	**-1.5**	*smoG*	Sorbitol/mannitol transport system ATP-binding protein
	Bmul_0712	**-1.4**	*mtlK*	Mannitol dehydrogenase domain
	Bmul_0897	**1.3**	*otsA*	alpha,alpha-trehalose-phosphate synthase (UDP-forming)
	Bmul_3783	**-1.7**	-	Periplasmic-binding protein
	Bmul_3784	**-1.3**	-	Monosaccharide-transporting ATPase
	Bmul_3785	**-1.5**	-	Monosaccharide-transporting ATPase

Amino acid	Bmul_0305	**-1.4**	*gltB*	Glutamate synthase (ferredoxin)
transport and	Bmul_0306	**-1.4**	*gltD*	Glutamate synthase, NADH/NADPH, small subunit
metabolism	Bmul_1255	**-1.2**	*glnD*	UTP-GlnB uridylyltransferase
	Bmul_2715	**-1.4**	*gdhA*	Glu-Leu-Phe-Val dehydrogenase
	Bmul_3721	**1.4**	*glnA*	Glutamine synthetase catalytic region

[1] LB-FC, lower bound of fold change; * only genes with a lower bound of fold change above 1.7 are shown. ** the *bce* genes shown are the ones with a lower bound of fold-change above 4.0.

REFERENCES

Altschul, S. F., Madden, T. L., Schaffer, A. A., Zhang, J., Zhang, Z., Miller, W. & Lipman, D. J. (1997). Gapped BLAST and PSI-BLAST: a new generation of protein database search programs. *Nucleic Acids Res* **25**, 3389-3402.

Aubert, D., MacDonald, D. K. & Valvano, M. A. (2010). BcsKC is an essential protein for the type VI secretion system activity in *Burkholderia cenocepacia* that forms an outer membrane complex with BcsLB. *J Biol Chem* **285**, 35988-35998.

Baldwin, A., Mahenthiralingam, E., Drevinek, P. & other authors (2007). Environmental *Burkholderia cepacia* complex isolates in human infections. *Emerg Infect Dis* **13**, 458-461.

Bauer, A. W., Kirby, W. M., Sherris, J. C. & Turck, M. (1966). Antibiotic susceptibility testing by a standardized single disk method. *Am J Clin Pathol* **45**, 493-496.

Burtnick, M., Bolton, A., Brett, P., Watanabe, D. & Woods, D. (2001). Identification of the acid phosphatase (*acpA*) gene homologues in pathogenic and non-pathogenic *Burkholderia* spp. facilitates TnphoA mutagenesis. *Microbiology* **147**, 111-120.

Bylund, J., Burgess, L. A., Cescutti, P., Ernst, R. K. & Speert, D. P. (2006). Exopolysaccharides from *Burkholderia cenocepacia* inhibit neutrophil chemotaxis and scavenge reactive oxygen species. *J Biol Chem* **281**, 2526-2532.

Coenye, T., Drevinek, P., Mahenthiralingam, E., Shah, S. A., Gill, R. T., Vandamme, P. & Ussery, D. W. (2007). Identification of putative noncoding RNA genes in the *Burkholderia cenocepacia* J2315 genome. *FEMS Microbiol Lett* **276**, 83-92.

Conway, B. A., Chu, K. K., Bylund, J., Altman, E. & Speert, D. P. (2004). Production of exopolysaccharide by *Burkholderia cenocepacia* results in altered cell-surface interactions and altered bacterial clearance in mice. *J Infect Dis* **190**, 957-966.

Costerton, J. W., Stewart, P. S. & Greenberg, E. P. (1999). Bacterial biofilms: a common cause of persistent infections. *Science* **284**, 1318-1322.

Cunha, M. V., Sousa, S. A., Leitão, J. H., Moreira, L. M., Videira, P. A. & Sá-Correia, I. (2004). Studies on the involvement of the exopolysaccharide produced by cystic fibrosis-associated isolates of the *Burkholderia cepacia* complex in biofilm formation and in persistence of respiratory infections. *J Clin Microbiol* **42**, 3052-3058.

Downey, D. G., Bell, S. C. & Elborn, J. S. (2009). Neutrophils in cystic fibrosis. *Thorax* **64**, 81-88.

Dufour, Y. S., Kiley, P. J. & Donohue, T. J. (2010). Reconstruction of the core and extended regulons of global transcription factors. *PLoS Genet* **6**, e1001027.

Ferreira, A. S., Leitão, J. H., Sousa, S. A., Cosme, A. M., Sá-Correia, I. & Moreira, L. M. (2007). Functional analysis of *Burkholderia cepacia* genes *bceD* and *bceF*, encoding a phosphotyrosine phosphatase and a tyrosine autokinase, respectively: role in exopolysaccharide biosynthesis and biofilm formation. *Appl Environ Microbiol* **73**, 524-534.

Ferreira, A. S., Leitão, J. H., Silva, I. N., Pinheiro, P. F., Sousa, S. A., Ramos, C. G. & Moreira, L. M. (2010). Distribution of cepacian biosynthesis genes among environmental and clinical *Burkholderia* strains and role of cepacian exopolysaccharide in resistance to stress conditions. *Appl Environ Microbiol* **76**, 441-450.

Govan, J. R. & Nelson, J. W. (1992). Microbiology of lung infection in cystic fibrosis. *Br Med Bull* **48**, 912-930.

Govan, J. R., Brown, P. H., Maddison, J., Doherty, C. J., Nelson, J. W., Dodd, M., Greening, A. P. & Webb, A. K. (1993). Evidence for transmission of *Pseudomonas cepacia* by social contact in cystic fibrosis. *Lancet* **342**, 15-19.

Hammond, J. P., Broadley, M. R., Craigon, D. J., Higgins, J., Emmerson, Z. F., Townsend, H. J., White, P. J. & May, S. T. (2005). Using genomic DNA-based probe-selection to improve the sensitivity of high-density oligonucleotide arrays when applied to heterologous species. *Plant Methods* **1**, 10.

He, J., Dai, X. & Zhao, X. (2007). PLAN: a web platform for automating high-throughput BLAST searches and for managing and mining results. *BMC Bioinformatics* **8**, 53.

Holden, M. T., Seth-Smith, H. M., Crossman, L. C. & other authors (2009). The genome of *Burkholderia cenocepacia* J2315, an epidemic pathogen of cystic fibrosis patients. *J Bacteriol* **191**, 261-277.

Hunt, T. A., Kooi, C., Sokol, P. A. & Valvano, M. A. (2004). Identification of *Burkholderia cenocepacia* genes required for bacterial survival in vivo. *Infect Immun* **72**, 4010-4022.

Huse, H. K., Kwon, T., Zlosnik, J. E., Speert, D. P., Marcotte, E. M. & Whiteley, M. (2010). Parallel evolution in *Pseudomonas aeruginosa* over 39,000 generations in vivo. *mBio* **1**.

Isles, A., Maclusky, I., Corey, M., Gold, R., Prober, C., Fleming, P. & Levison, H. (1984). *Pseudomonas cepacia* infection in cystic fibrosis: an emerging problem. *J Pediatr* **104**, 206-210.

Korner, H., Sofia, H. J. & Zumft, W. G. (2003). Phylogeny of the bacterial superfamily of Crp-Fnr transcription regulators: exploiting the metabolic spectrum by controlling alternative gene programs. *FEMS Microbiol Rev* **27**, 559-592.

Leitão, J. H., Sousa, S. A., Ferreira, A. S., Ramos, C. G., Silva, I. N. & Moreira, L. M. (2010). Pathogenicity, virulence factors, and strategies to fight against *Burkholderia cepacia* complex pathogens and related species. *App Microbiol Biotechnol* **87**, 31-40.

Li, C. & Wong, W. H. (2001a). Model-based analysis of oligonucleotide arrays: model validation, design issues and standard error application. *Genome Biol* **2**, RESEARCH0032.

Li, C. & Wong, W. H. (2001b). Model-based analysis of oligonucleotide arrays: expression index computation and outlier detection. *Proc Natl Acad Sci U S A* **98**, 31-36.

Mahenthiralingam, E., Urban, T. A. & Goldberg, J. B. (2005). The multifarious, multireplicon *Burkholderia cepacia* complex. *Nat Rev Microbiol* **3**, 144-156.

Martin, D. W., Schurr, M. J., Mudd, M. H., Govan, J. R., Holloway, B. W. & Deretic, V. (1993). Mechanism of conversion to mucoidy in *Pseudomonas aeruginosa* infecting cystic fibrosis patients. *Proc Natl Acad Sci U S A* **90**, 8377-8381.

McKeon, S. A., Nguyen, D. T., Viteri, D. F., Zlosnik, J. E. & Sokol, P. A. (2011). Functional quorum sensing systems are maintained during chronic *Burkholderia cepacia* complex infections in patients with cystic fibrosis. *J Infect Dis* **203**, 383-392.

Moreira, L. M., Da Costa, M. S. & Sá-Correia, I. (1997). Comparative genomic analysis of isolates belonging to the six species of the genus *Thermus* using pulsed-field gel electrophoresis and ribotyping. *Arch Microbiol* **168**, 92-101.

Moreira, L. M., Videira, P. A., Sousa, S. A., Leitão, J. H., Cunha, M. V. & Sá-Correia, I. (2003). Identification and physical organization of the gene cluster involved in the biosynthesis of *Burkholderia cepacia* complex exopolysaccharide. *Biochem Biophys Res Commun* **312**, 323-333.

Nzula, S., Vandamme, P. & Govan, J. R. (2002). Influence of taxonomic status on the in vitro antimicrobial susceptibility of the *Burkholderia cepacia* complex. *J Antimicrob Chemother* **50**, 265-269.

Oliver, A., Canton, R., Campo, P., Baquero, F. & Blazquez, J. (2000). High frequency of hypermutable *Pseudomonas aeruginosa* in cystic fibrosis lung infection. *Science* **288**, 1251-1254.

Pedersen, S. S., Hoiby, N., Espersen, F. & Koch, C. (1992). Role of alginate in infection with mucoid *Pseudomonas aeruginosa* in cystic fibrosis. *Thorax* **47**, 6-13.

Pfaffl, M. W. (2001). A new mathematical model for relative quantification in real-time RT-PCR. *Nucleic Acids Res* **29**, e45.

Rau, M. H., Hansen, S. K., Johansen, H. K. & other authors (2010). Early adaptive developments of *Pseudomonas aeruginosa* after the transition from life in the environment to persistent colonization in the airways of human cystic fibrosis hosts. *Environ Microbiol* **12**, 1643-1658.

Sambrook, J., and D.W. Russell (2001). *Molecular cloning: a laboratoty manual*. New York: CSHL Press.

Schwarz, S., Hood, R. D. & Mougous, J. D. (2010). What is type VI secretion doing in all those bugs? *Trends Microbiol* **18**, 531-537.

Seed, K. D. & Dennis, J. J. (2008). Development of *Galleria mellonella* as an alternative infection model for the *Burkholderia cepacia* complex. *Infect Immun* **76**, 1267-1275.

Smith, E. E., Buckley, D. G., Wu, Z. & other authors (2006). Genetic adaptation by *Pseudomonas aeruginosa* to the airways of cystic fibrosis patients. *Proc Natl Acad Sci U S A* **103**, 8487-8492.

Sousa, S. A., Ulrich, M., Bragonzi, A. & other authors (2007). Virulence of *Burkholderia cepacia* complex strains in gp91$^{phox-/-}$ mice. *Cell Microbiol* **9**, 2817-2825.

Taylor, B. L. (2007). Aer on the inside looking out: paradigm for a PAS-HAMP role in sensing oxygen, redox and energy. *Mol Microbiol* **65**, 1415-1424.

Zlosnik, J. E., Hird, T. J., Fraenkel, M. C., Moreira, L. M., Henry, D. A. & Speert, D. P. (2008). Differential mucoid exopolysaccharide production by members of the *Burkholderia cepacia* complex. *J Clin Microbiol* **46**, 1470-1473.

Zlosnik, J. E. & Speert, D. P. (2010). The role of mucoidy in virulence of bacteria from the *Burkholderia cepacia* complex: a systematic proteomic and transcriptomic analysis. *J Infect Dis* **202**, 770-781.

Zlosnik, J. E., Costa, P. S., Brant, R., Mori, P. Y., Hird, T. J., Fraenkel, M. C., Wilcox, P. G., Davidson, A. G. & Speert, D. P. (2011). Mucoid and Nonmucoid *Burkholderia cepacia* complex bacteria in cystic fibrosis infections. *Am J Respir Crit Care Med* **183**, 67-72.

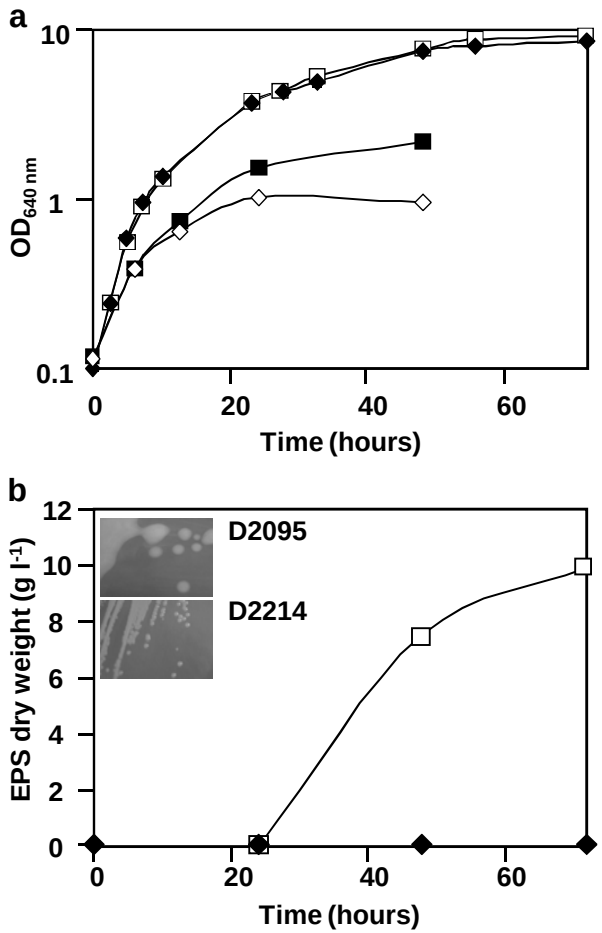
a
10
1
0.1
OD640 nm
0
20
40
60
Time (hours)
b
12
10
8
6
4
2
0
EPS dry weight (g l-1)
D2095
D2214
0
20
40
60
Time (hours)

Figure 1

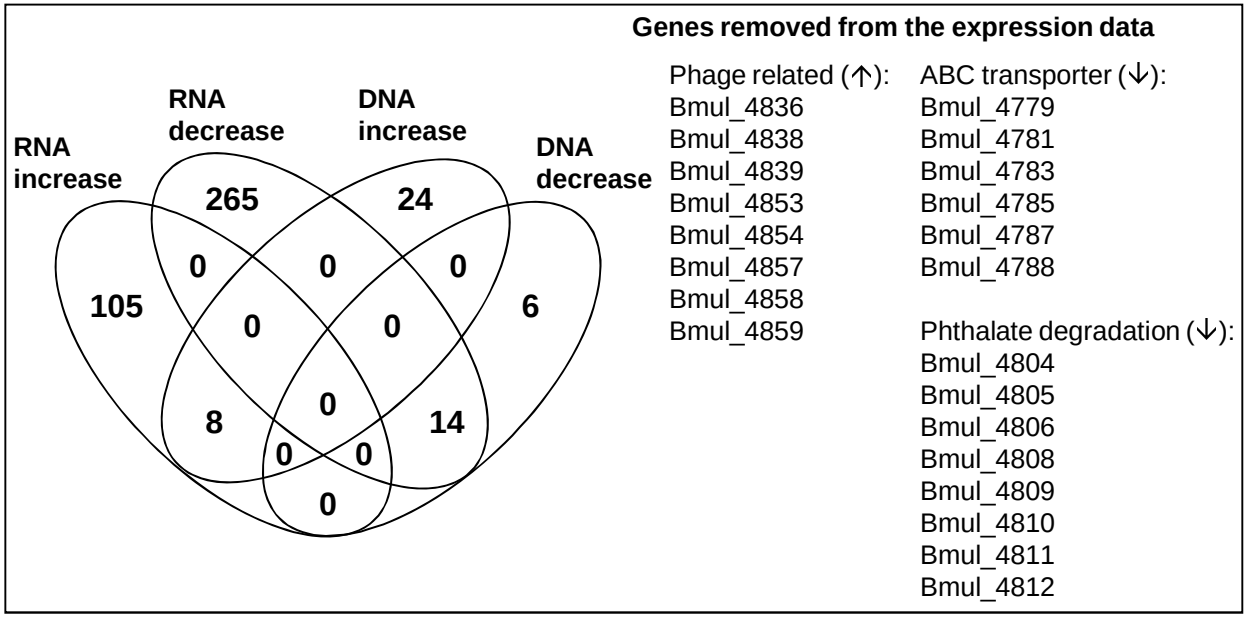

Genes removed from the expression data

Phage related (↑):
Bmul_4836
Bmul_4838
Bmul_4839
Bmul_4853
Bmul_4854
Bmul_4857
Bmul_4858
Bmul_4859

ABC transporter (↓):
Bmul_4779
Bmul_4781
Bmul_4783
Bmul_4785
Bmul_4787
Bmul_4788

Phthalate degradation (↓):
Bmul_4804
Bmul_4805
Bmul_4806
Bmul_4808
Bmul_4809
Bmul_4810
Bmul_4811
Bmul_4812

Figure 2

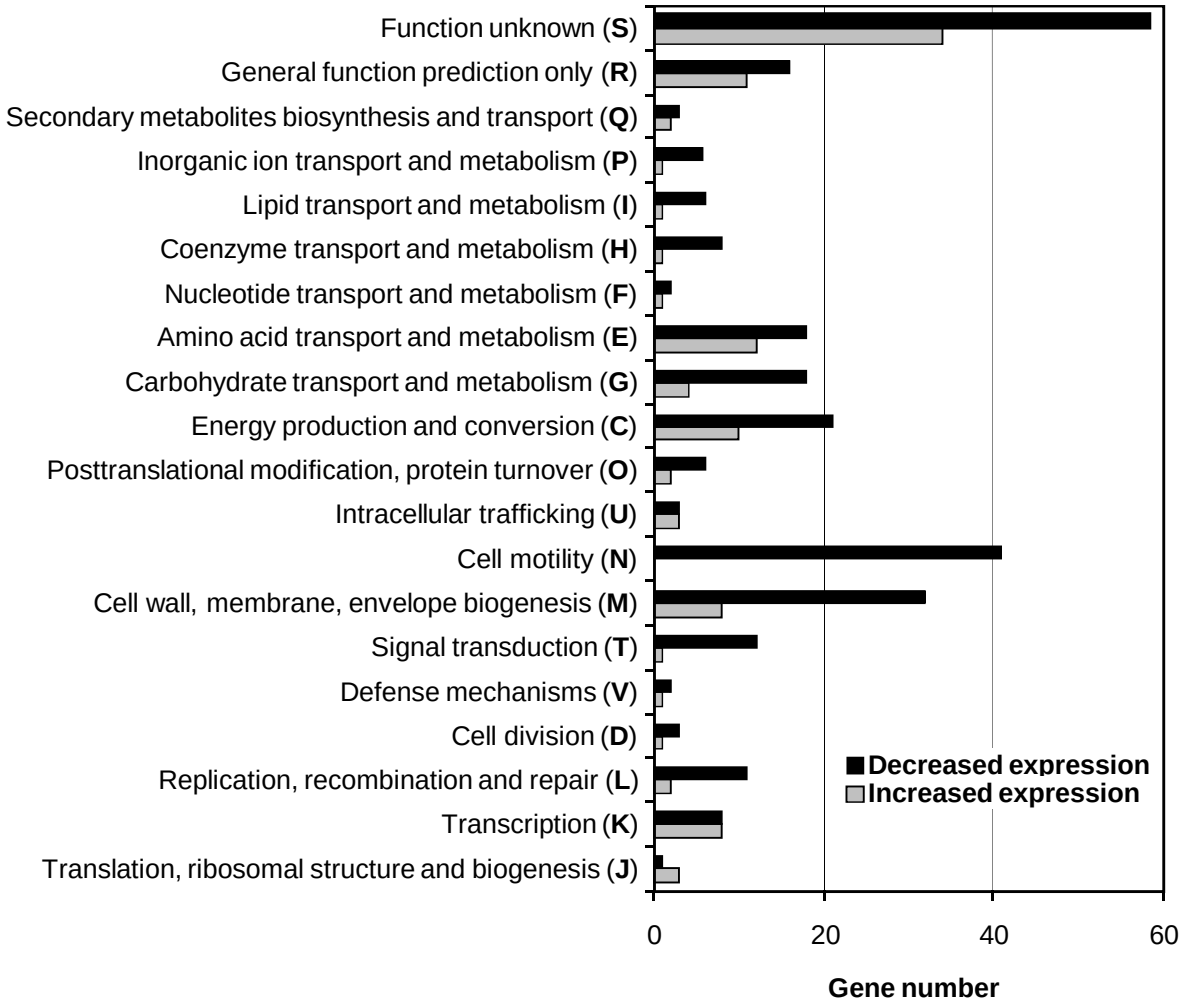
Function unknown (S)
General function prediction only (R)
Secondary metabolites biosynthesis and transport (Q)
Inorganic ion transport and metabolism (P)
Lipid transport and metabolism (I)
Coenzyme transport and metabolism (H)
Nucleotide transport and metabolism (F)
Amino acid transport and metabolism (E)
Carbohydrate transport and metabolism (G)
Energy production and conversion (C)
Posttranslational modification, protein turnover (O)
Intracellular trafficking (U)
Cell motility (N)
Cell wall, membrane, envelope biogenesis (M)
Signal transduction (T)
Defense mechanisms (V)
Cell division (D)
Replication, recombination and repair (L)
Transcription (K)
Translation, ribosomal structure and biogenesis (J)
Decreased expression
Increased expression
0
20
40
60
Gene number

Figure 3

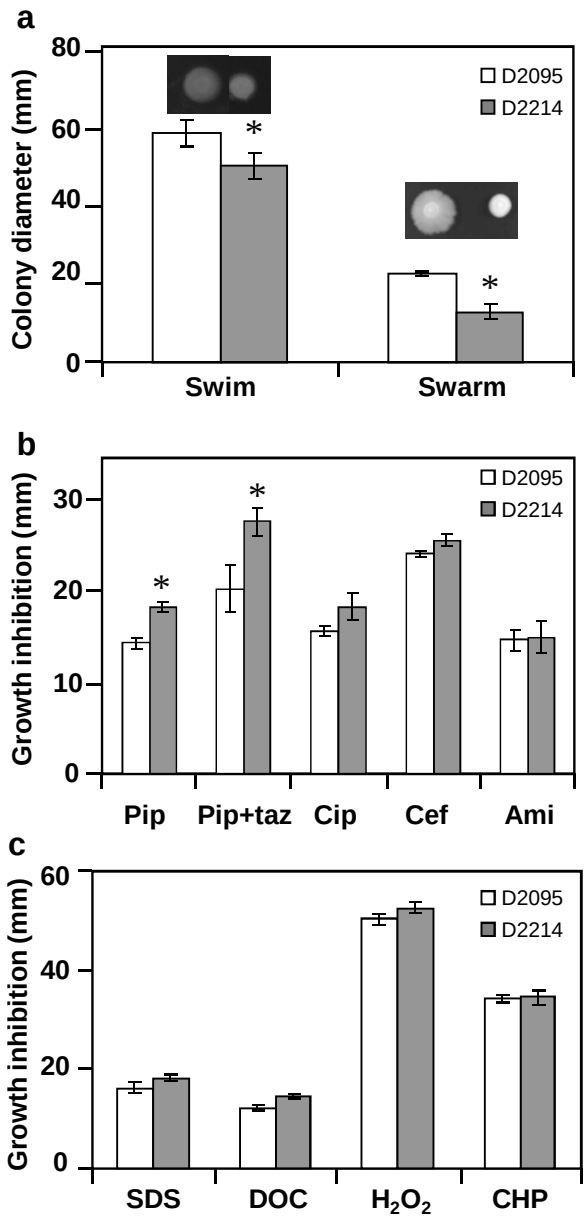
a
Colony diameter (mm)
80
60
40
20
0
D2095
D2214
*
*
Swim
Swarm
b
Growth inhibition (mm)
30
20
10
0
D2095
D2214
*
*
Pip
Pip+taz
Cip
Cef
Ami
c
Growth inhibition (mm)
60
40
20
0
D2095
D2214
SDS
DOC
H2O2
CHP

Figure 4

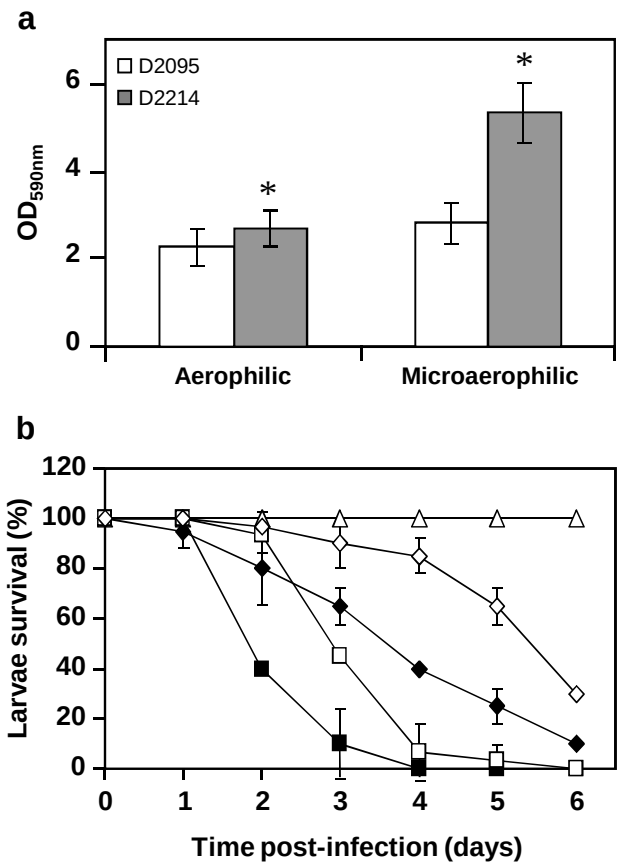
a
D2095
D2214
OD_{590nm}
0
2
4
6
*
*
Aerophilic
Microaerophilic
b
Larvae survival (%)
0
20
40
60
80
100
120
0
1
2
3
4
5
6
Time post-infection (days)

Figure 5

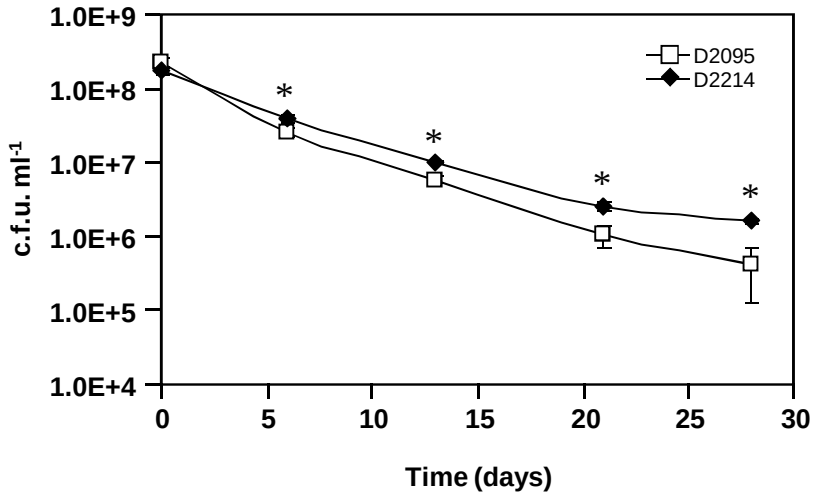
1.0E+9
1.0E+8
1.0E+7
1.0E+6
1.0E+5
1.0E+4
c.f.u. ml-1
0
5
10
15
20
25
30
Time (days)
D2095
D2214
*
*
*
*

Figure 6